Very-low-frequency Raman scattering in vitreous silica*

G. Winterling
Max-Planck-Institut für Festkörperforschung, Stuttgart, Federal Republic of Germany
(Received 18 February 1975)

The very-low-frequency Raman scattering from vitreous silica was measured for frequency shifts ω as small as 4 cm^{-1}. The data were compared with present theories on disorder-induced sacttering; for $\omega < 20$ cm^{-1} an excess scattered intensity was found, which is not seen in the corresponding crystalline state. The magnitude of this excess intensity was determined relative to that of the Brillouin lines; its temperature dependence was found to be stronger than one-phonon processes, but weaker than two-phonon processes. We discuss the excess scattering in terms of existing models for the low-temperature specific heat of glasses and find, at least for temperatures $T > 80$ K, our data to be consistent with disorder-induced scattering from damped high-frequency sound waves.

I. INTRODUCTION

Recently, glasses have gained a renewed interest because of their anomalous thermal properties at very low temperatures ($T < 2$ K).[1-3] The excess specific heat, being dominated by a term varying linearly with temperature, indicates the presence of states in addition to the (long-wavelength) Debye phonons. The physical nature of these additional states is still unclear and represents a problem of current interest.

Fulde and Wagner[4] have proposed that a structural relaxation is mainly responsible for the anomalous thermal properties of the glasses. This relaxation leads to an increased damping of the acoustic phonons and to a low-frequency tail in the spectral function of these phonons. At very low temperatures, the large-momentum phonon states—in general frozen out in the crystalline solid—can still be partially occupied through their low-frequency tails, thereby giving rise to the excess specific heat.

Anderson, Halperin, and Varma[5] (AHV) and, independently, Phillips[6] have advanced a more specific model for the structural defects of a glass. They assume that in a glass, atoms or a group of atoms may have two almost equivalent equilibrium positions which are described by a double-well potential. For atoms where the potential is not too asymmetric and the central barrier not too high, transitions between the upper and lower level, even at low temperatures, can occur by phonon-assisted tunneling. According to this model, the excess specific heat is a direct measure of the number density of these two-level systems.

Using the model of AHV, Jäckle[7] was able to quantitatively predict the saturation of sound attenuation which had been proposed earlier[8] and which was subsequently verified in ultrasonic experiments.[9] Although these experiments have demonstrated the usefulness of the model of AHV, its generality has been questioned[2] in view of the fact that a variety of glasses show, in spite of great differences in their chemical compositions, thermal anomalies of quite comparable magnitude.

The present investigation is mainly motivated by the question of whether light-scattering experiments can provide additional information on the states responsible for the excess specific heat. As far as we know, previous experiments[10] did not contain any observation of these states and good Raman data[11-13] have only been available for frequency shifts larger than 15 cm^{-1}. In principle, however, light scattering can only be fruitful if these states couple to the light with sufficient strength.

In this paper, we report a detailed investigation of the low-frequency Raman spectrum of vitreous silica down to frequency shifts ω of 4 cm^{-1}. We compare our data with current theories of disorder-induced scattering,[14-16] which based on a Debye model, predict that the low-frequency scattered intensity should vanish for $\omega \to 0$. In contrast to this theoretical prediction, our data exhibit a significant finite scattered intensity for $\omega \to 0$, indicating an "excess" scattering. We have measured not only the temperature variation of this "excess" contribution from room temperature down to 40 K, but also its depolarization ratio and its magnitude relative to the Brillouin lines. We present arguments that the excess contribution cannot be accounted for by the high-frequency tails of the Brillouin lines nor by scattering processes of second order. The excess scattering is discussed in terms of the models proposed for the excess specific heat.

II. EXPERIMENT AND RESULTS

The Raman spectra were recorded by using both an argon-ion laser (514 nm) and a krypton laser (647 nm) as exciting light sources, and a Jarrell-Ash double-grating spectrometer followed by standard photon counting equipment. A 90°, scattering

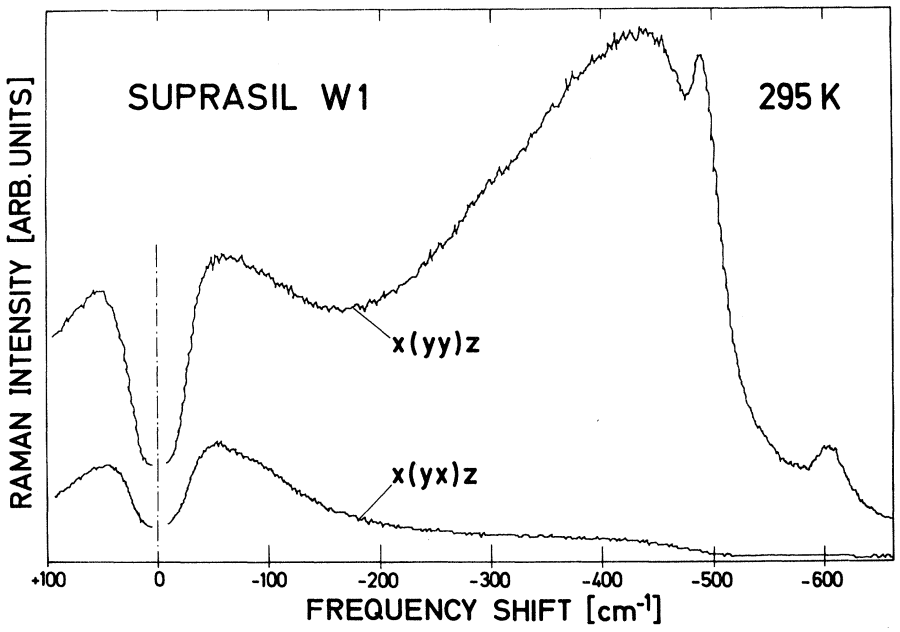

FIG. 1. Raman spectra of vitreous silica (Suprasil *W*1). The upper and lower curves represent the polarized and depolarized scattering, respectively.

geometry was employed with $f/2$ collection optics, and care was taken that no parasitic stray light, mostly originating from the sample surfaces, could enter the spectrometer. The change of the spectral sensitivity of our detection system—depending on photomultiplier sensitivity and grating efficiency—was measured at 514 nm by recording the first-order Raman scattering of crystalline quartz. The response was found to increase by about 18% when going from 128 cm^{-1} on the Stokes side to 128 cm^{-1} on the anti-Stokes side. The polarization dependence of the spectrometer transmission was compensated by inserting a polarization scrambler in front of the entrance slit.

Figure 1 shows the polarized and depolarized Raman spectra of the vitreous silica Suprasil *W*1, (Ref. 17) for $T = 295$ K. These spectra are included here as a reminder of the general features at higher frequencies already discussed in the literature.[11–13]. The strongly polarized character of the spectrum for $\omega > 200$ cm^{-1} is typical; at smaller frequency shifts the depolarization ratio is increasing, and for $\omega < 120$ cm^{-1} polarized and depolarized spectra exhibit practically the same spectral shape. For $\omega < 50$ cm^{-1} the scattered intensity decreases with decreasing ω. Our very-low-frequency data of the depolarized scattering, as displayed in Fig. 2 for Suprasil 1 (Ref. 17) indicate a minimum of the

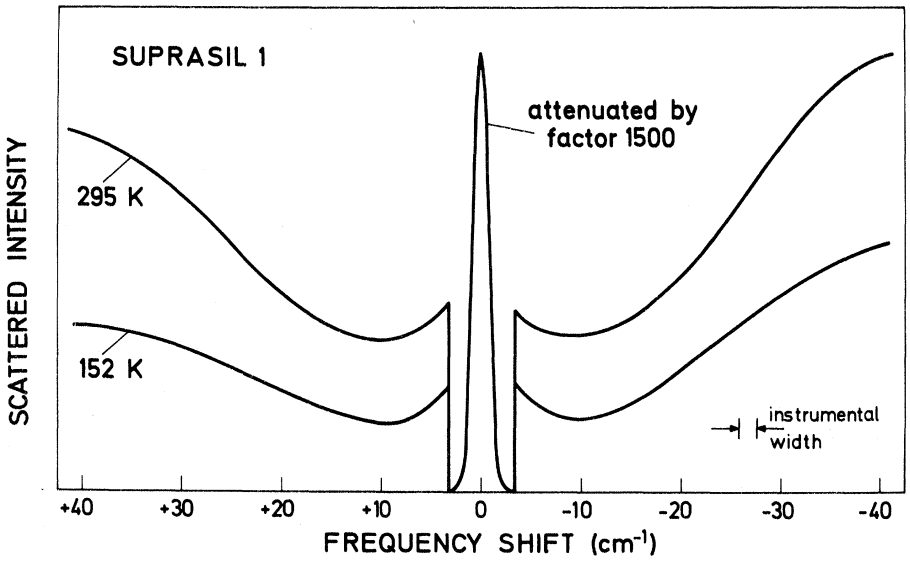

FIG. 2. Depolarized scattering from vitreous silica (Suprasil 1) excited with 514 nm. The curve at $T = 152$ K was normalized relative to that at $T = 295$ K at $\omega = -420$ cm^{-1}, assuming one-phonon processes.

scattered intensity around $\omega \simeq 10$ cm^{-1} and an increase for $\omega < 10$ cm^{-1}. This increase was found in both types of Suprasil investigated; however, it is more pronounced in the sample of Suprasil 1, which in contrast to Suprasil *W*1, has a rather high concentration of OH^- on the order of 1000 ppm.

The finite scattered intensity for $\omega \to 0$ required a careful investigation of the instrumental profile. Under our experimental conditions, the contrast $I_{\text{tail}}/I_{\text{peak}}$ was found to be, for example, 2.7×10^{-6} at $\omega = -5$ cm^{-1} when using the 514-nm line and even one order of magnitude better (for example, 4.1×10^{-7} at $\omega = -4$ cm^{-1}) when measuring with the 647-nm line. The depolarized Raman scattering at 5 cm^{-1} on the other hand, is at room temperature about 2.6×10^{-4} times the scattered intensity at $\omega = 0$ (for 514 nm), thereby being still two orders of magnitude stronger than the instrumental tail of the elastic Rayleigh scattering. In the red, the experimental situation is even better, and Raman data can be taken as close as 4 cm^{-1} to the exciting line. It should be noted that the experimental conditions here are much more favorable than with opaque amorphous semiconductors[18] where, in general, the large stray light contribution from the sample surface masks the intrinsic spectrum very close to the exciting line.

We were also able to spectrally resolve the central line of the scattering spectrum (see Fig. 2) by drastically reducing the width and height of the spectrometer slits. In this case, with a reduced instrumental width of 0.4 cm^{-1}, the ratio of the polarized intensities of one Brillouin line (scattering from longitudinal phonons) to the Rayleigh line was measured at $T = 295$ K to be $\simeq 0.021$ (at 514 nm), which agrees well with the value obtained earlier with a Fabry-Perot interferometer.[19] We further determined, to our knowledge for the first time in an amorphous solid, the magnitude of the (disorder-allowed) Raman background relative to the (k-allowed) Brillouin scattering. The polarized Raman intensity at $\omega = -6$ cm^{-1} (within one instrumental width of 1.9 cm^{-1}) was found to be $(1.3\pm0.3)\times10^{-3}$ times the integrated intensity of one polarized Brillouin line at $T = 295$ K, using 514-nm light.

The depolarization ratio I_{xy}/I_{yy} of the Raman scattering at room temperature was found to be frequency independent in the investigated frequency interval $6 < \omega < 40$ cm^{-1} and to have a value of 0.30 ± 0.03, which is about three times larger than the calculated depolarization ratio of 0.094 for the Brillouin scattering (see Appendix A and Ref. 20). Combining these two numbers, the intensity ratio of the depolarized Raman scattering at 6 cm^{-1} to one depolarized Brillouin line is computed to be $(4.3\pm1)\times10^{-3}$.

Finally, we measured the temperature dependence of the Raman scattering in Suprasil *W*1 from 295 to 40 K. The corresponding data are shown in Fig. 4.

III. DISCUSSION OF THE DISORDER-INDUCED SCATTERING

It has been realized for some time that the Raman scattering from quartz in the frequency region around 50 cm^{-1} is much larger in the glassy state than in the crystalline state.[11–13] Whereas earlier interpretations[11,13] considered this finding as an indication for low-lying optical modes, it is now believed that the low-frequency Raman spectrum ($\omega < 50$ cm^{-1}) is dominantly due to a disorder-induced scattering from high-frequency sound waves. Whalley and Bertie[14] have discussed the consequences of orientational or electrical disorder which manifests itself as a spatially fluctuating polarizability. A sound wave with large momentum can, although weakly, take part in light scattering through combination with a particular (large-momentum) Fourier component of the photoelastic constant so that there arises a contribution to the dielectric tensor varying spatially with the (small) scattering wave vector.

Shuker and Gammon[15] have pointed out the consequences of the mechanical disorder which leads to a localization of the higher-frequency vibrations and, correspondingly, to finite Fourier components of the displacement at small wave vectors. Recently, Martin and Brenig[16] have developed a continuum model for the disorder-induced scattering from high-frequency sound waves. They consider both the electrical and mechanical disorder by introducing fluctuating contributions to the photoelastic and elastic constants. Their theory yields an approximate expression for the depolarization ratio I_{yx}/I_{yy}, depending on the sound velocities and the photoelastic constants. For vitreous silica, I_{yx}/I_{yy} is calculated for lower frequencies ($\omega < 30$ cm^{-1}) (see Appendix A) to be $\simeq 0.28$, which is close to the value observed in our experiment and which is also compatible with the Raman spectra of Ref. 12.

In general, the Raman intensity of the disorder-induced scattering can be written[15]

$$J_R(\omega, T) \propto \sum_b c_b(\omega)\rho_b(\omega)\left(\frac{n(\omega, T)+\binom{1}{0}}{\omega}\right). \qquad (1)$$

Here, c_b is the frequency-dependent coupling constant for the branch b, $\rho_b(\omega)$ is the density of states in branch b, and n is the thermal occupation number of a harmonic oscillator. The 1 and 0 in the parentheses refer to the Stokes and anti-Stokes spectrum, respectively. One basic assumption underlying Eq. (1) is that the vibrational states taking part in the scattering are narrow in the frequency domain.

According to Eq. (1), the temperature depen-

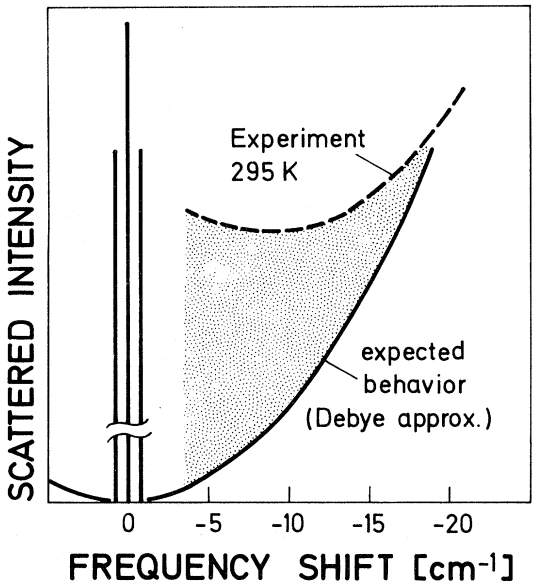

FIG. 3. Schematic of the (depolarized or polarized) spectrum of the light scattered at very-low-frequency shifts. The inner three lines represent the Rayleigh line and the Brillouin doublet, the full curve represents the weak Raman background expected from the theories of Refs. 14 and 16, the shaded area represents the excess scattering.

dence of the disorder-induced scattering is that of harmonic oscillators, which is in agreement with both our data for $|\omega| > 20$ cm^{-1} and with the earlier Raman data of Refs. 12 and 13 obtained for $|\omega| > 25$ cm^{-1}. The factor $(n+\frac{1}{0})\omega^{-1}$ in Eq. (1) is proportional to the mean square displacement of a vibrational mode with eigenfrequency ω. At low frequencies ($\omega < 50$ cm^{-1}),[21] the dominant contributions are expected to arise from modes having sound-wave character. The modulation of the dielectric tensor by a sound wave is, for a given displacement amplitude, larger, the larger the wavevector q. In the continuum limit—$2\pi/q$ much greater than the short-range correlation length ξ ($\xi \simeq 6.4$ Å for vitreous silica[22])—the coupling constant c_b of Eq. (1) can be shown to be proportional to q^2, and assuming a linear dispersion $\omega \propto q$, c_b is expected[14,16] to vary as

$$c_b \propto \omega^2 . \tag{2}$$

Recent experiments on amorphous silicon[18] are in agreement with this prediction. Thus, the scattered intensity at room temperature and very low frequencies ($\omega/2\pi \leq \frac{1}{10} v/\xi \approx 20$ cm^{-1} for vitreous silica[22]) should be roughly proportional to the density of states ρ_b, since $n(\omega, T) \simeq kT/\hbar\omega \gg 1$ under these conditions.

Describing the very-low-frequency excitations with a Debye model, the disorder-induced scattering is expected to vanish for $\omega \to 0$ roughly[14,16] as ω^2 (see Fig. 3). Even if the coupling constant c_b varies more weakly than ω^2, the scattering should vanish for $\omega \to 0$ because of the frequency dependence of the Debye density of states.

In contrast to that expectation, the measured Raman intensities—both for the polarized and depolarized scattering—do not vanish for $\omega \to 0$, as can be seen in Figs. 2 and 3. Therefore, we must conclude from our analysis based on Eqs. (1) and (2) that there is an excess scattered intensity (marked in Fig. 3 as the shaded area) in the Raman spectrum of vitreous silica. This excess intensity has the following properties: (a) It is characteristic of the glassy state of SiO_2, since the scattering from crystalline quartz in the same frequency region ($4 < \omega < 20$ cm^{-1}) is about one order of magnitude smaller. (b) It peaks for $\omega \sim 0$ within the resolution of our instrument. (c) Its magnitude at 5 cm^{-1} within one instrumental width of 1.9 cm^{-1} is about 1000 times weaker at $T = 295$ K than one polarized Brillouin line. (d) Its temperature dependence is stronger than that of harmonic oscillators, as can be seen from Fig. 4.

IV. DISCUSSION OF THE EXCESS SCATTERING

First, we would like to briefly discuss the excess scattering with respect to second-order processes

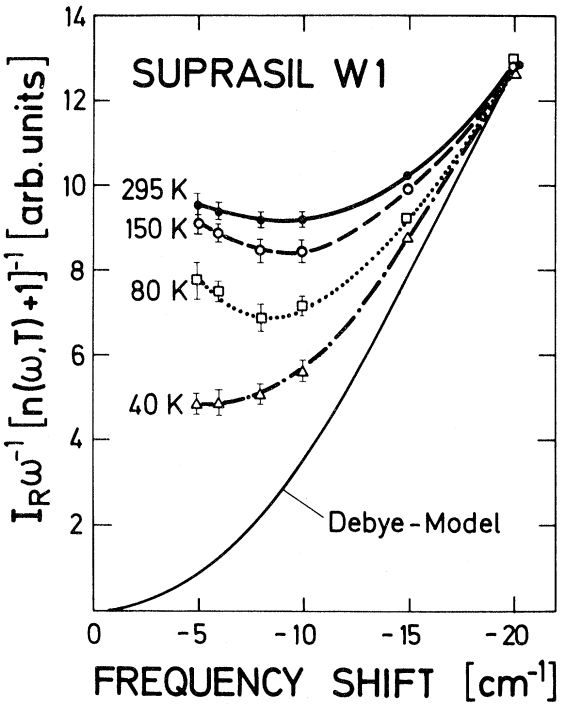

FIG. 4. Experimental Raman data dependent on temperature; the data were normalized at $\omega = -420$ cm^{-1} according to one-phonon processes. The theoretical expectation according to a Debye model is included for comparison.

and the high-frequency tails of the Brillouin lines, i.e., mechanisms which could also be present in the crystalline state. Second, we shall consider the excess scattering with respect to scattering from structural defects and damped high-frequency sound waves, i.e., mechanisms which are more characteristic of the glassy state.

A. Brillouin line shapes

In fused quartz, the damping of sound waves with frequencies $\omega/2\pi \sim 10^{10}$ Hz is determined at higher temperatures mainly by relaxation processes.[23,24] Describing this damping with one average relaxation time τ— a generalization to a distribution of relaxation times will not change our main arguments —the spectral function $S(q, \omega)$ of the Brillouin lines can be expressed in terms of the elastic response function $D(q, \omega)$[4,25] by

$$S(q, \omega) \propto c(q)\hbar\omega[n(\omega, T)+(\tfrac{1}{0})]\omega^{-1}\mathrm{Im}D(q, \omega)\,, \quad (3)$$

$$D(q, \omega) = \{\omega^2 - \omega_0^2(q)\,[1 - ig\omega\tau(1 - i\omega\tau)^{-1}\,]\}^{-1}\,, \quad (4)$$

and the coupling constant $c(q) \propto q^2$, with v being the sound velocity, and $\omega_0(q) = vq$. The constant g describes the strength of the relaxation and is related to the high- and low-frequency limit of the sound velocity by

$$v_\infty^2 = v_0^2(1+g)\,. \quad (5)$$

The above hydrodynamic description is similar to liquids where the relaxation between the translational and internal degrees of freedom is commonly described in terms of a frequency-dependent bulk viscosity. It is instructive to consider the line shapes for the high-frequency ($\omega_0\tau \gg 1$) and the low-frequency ($\omega_0\tau \ll 1$) limits. For the second case, we obtain from Eqs. (3) and (4), assuming $g \ll 1$ and $\hbar\omega/kT \ll 1$,

$$S(q, \omega) \propto \frac{\Gamma(q)\omega_0^2(q)}{[\omega^2 - \omega_0^2(q)]^2 + \Gamma^2(q)\omega^2}\,, \quad (6)$$

where $\Gamma \equiv \omega_0^2(q)g\tau$ is the full width at half-height (FWHH) of a Brillouin line. For frequency shifts $\omega^2 \gg \omega_0^2$, the spectral function S rolls off like $\sim \Gamma\omega^{-4}$, whereas at the low-frequency side, $S(q, \omega)$ exhibits a long tail, as is schematically sketched in Fig. 5(a). In the other limit $\omega_0\tau \gg 1$, this tail separates off the main line and appears as a central mode [see Fig. 5(b)], the strength and width of which are determined by the relaxation strength g and the relaxation rate τ^{-1}, respectively. The main line is approximately Lorentzian for frequencies $\omega \approx \omega_\infty$.

In our experiment using 514-nm light, the Brillouin lines of the transverse and longitudinal sound waves are at frequency shifts of 0.49 and 0.77 cm^{-1}, respectively. The high-frequency tail of the stronger 0.77-cm^{-1} line at 5 cm^{-1} is estimated from Eq. (6) and the damping data of Ref. 23 to be weaker than the observed scattered intensity at 5 cm^{-1} by about three orders of magnitude. Also, since the depolarization ratio of the excess scattering is much different from that of the Brillouin scattering, the excess scattering observed (see Fig. 3) cannot arise from the high-frequency tails of the Brillouin scattering. An analysis of the experimental Brillouin lines shape by Sandercock[26] strongly supports this conclusion.

B. Second-order scattering

From crystals it is known that second-order scattering, particularly difference processes, may contribute to the scattering at small frequency shifts. These processes, however, have a temperature dependence proportional to $n_1(\Omega_1, T) \times [1 + n_2(\Omega_2' T)]$ with $\omega = |\Omega_2 - \Omega_1|$, which is much stronger than that of first-order scattering. For example, for $\omega = 5$-cm^{-1} second-order scattering at $T = 80$ K would be weaker by at least a factor of 0.08 than its value at $T = 295$ K; the experimental values for the scattering, in contrast, have the larger ratio of 0.22 (see also Fig. 4), so that second-order processes cannot account for the observed temperature dependence of the excess scat-

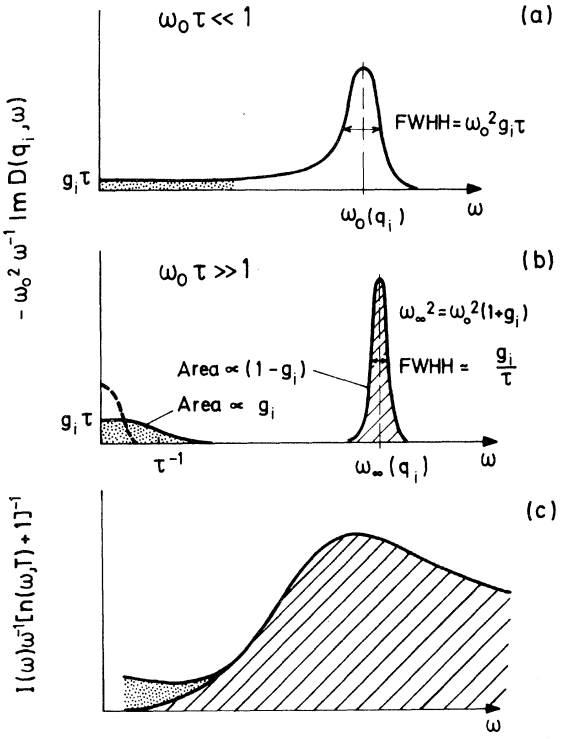

FIG. 5. Expected line shapes for the scattering from state q_i are sketched in (a) and (b) for the low-frequency and high-frequency limits, respectively. FWHH denotes the full width at half-height. The disorder-induced spectrum obtained by summation over all states q_i is sketched in (c).

tering. In addition, second-order scattering of comparable strength is not known in crystalline quartz for $\omega < 100$ cm^{-1}.

C. Damped high-frequency sound waves

The thermal conductivity data[1,2] tell us that the acoustic phonons in fused quartz are much more strongly damped than in crystalline quartz. Consequently, the description of the disorder-induced scattering in terms of vibrations narrow in frequency domain, as discussed in Sec. III, [14–16] is only a rough approximation; in particular, phonons with high momentum q may possess a low-frequency tail in their spectral function. These tails, although weak in comparison to the main spectral density near $\omega \sim v(q)q$, can give a remarkable contribution to the scattering for $\omega \to 0$, due to their large density of states. In this respect, strong damping of acoustic phonons may account for the observed excess scattering, its temperature dependence, and also for an excess specific heat.[4] This interpretation is further supported by the fact that the excess scattering shows the same depolarization ratio as the Raman scattering at higher-frequency shifts ($15 < \omega < 40$ cm^{-1}).

In order to obtain an approximate description of the high-momentum excitations — no theoretical model specific for the glassy state is known to us at present —we extend the hydrodynamic description[4] of Eq. (4) to large values of q. Each state, characterized with its $\vec{q}$ value can contribute to the disorder-induced scattering depending on the value of the coupling constant $c_b(|\vec{q}|)$. The spectrum of the scattered light is obtained by summing up the contributions of all states $\vec{q}_i$,

$$I(\omega) \propto \sum_{\vec{q}_i} c(|\vec{q}_i|)\,[n(\omega, T) + (\tfrac{1}{0})]\,\mathrm{Im}D(|\vec{q}_i|, \omega)\ . \quad (7)$$

$D(q_i, \omega)$, as defined in Eq. (4), may be generalized to include several relaxation processes by replacing in the denominator $g\omega\tau(1 - i\omega\tau)^{-1}$ with $\sum_m g_m \omega\tau_m \times (1 - i\omega\tau_m)^{-1}$. For $g_m = 0$, Eq. (7) reduces to Eq. (1).

In order to allow comparison with the experimental data of Fig. 4, we rewrite Eq. (7),

$$\frac{I(\omega)}{\omega[n(\omega, T)+1]} \propto \sum_{\vec{q}_i} c_b(q_i)\omega^{-1}\,\mathrm{Im}D(q_i, \omega)\ . \quad (8)$$

The spectral shape of one term in the sum has already been discussed above for one relaxation process and is displayed in Figs. 5(a) and 5(b). Although neither the dispersion $\omega_0 = \omega_0(q_i)$ nor the coupling constant $c_b(q_i)$ are known for large values of q, information on the parameters of the relaxation process can be obtained from our data in the following way: The sum over the main spectral weights located near $\omega \simeq \omega_0(q_i)$ of all terms is proportional to the density of states in the long-wavelength limit, i.e., $\omega < 20$ cm^{-1}. For frequency shifts $20 < \omega < 120$ cm^{-1}, this sum is expected to be proportional to the measured spectrum divided by $\omega[n(\omega, T) + (\frac{1}{0})]$; hence, this sum can be represented in Fig. 5(c) by the curve enclosing the dashed area. The low-frequency tails of Figs. 5(a) and 5(b), always weighted with the corresponding coupling factor $c(q_i)$, should add up to the dotted area in Fig. 5(c). From Figs. 5(a) and 5(b), it is evident for frequencies $\omega < \omega_0(q)$ that with decreasing relaxation rate τ^{-1}, the tail contributions increase for $\omega < \tau^{-1}$ but, decrease for $\omega > \tau^{-1}$.

We may now compare our experimental data of Fig. 4, in particular, the decrease of the "excess" scattering[27] with decreasing temperature, with the theoretical expectation of Fig. 5. The decrease of the tail contribution for $5 < \omega < 20$ cm^{-1} suggests that the average relaxation rate τ_1^{-1} of the dominant relaxation process is smaller than $\omega \approx 5$ cm^{-1} ($\approx 10^{12}$ sec^{-1}) at $T = 150$ K and is further decreasing with decreasing temperature; at $T = 40$ K, this relaxation process is practically no longer seen in our data, which indicates that it has become very narrow in frequency. The remaining "excess" scattering at 40 K may be explained in this context by assuming another relaxation process,[7,28,29] which is considerably faster than the first process. The relaxation strength g is obtained for $\omega_0\tau \gg 1$ as the ratio of the dotted to the dashed area [see Fig. 5(b)]. Comparing Fig. 5(c) with the experimental data[30] (see Figs. 1 and 4) which are extrapolated to $\omega \simeq 0$ following the given curvature, the strength g_1 of the first process at $T = 150$ K is estimated to be $g_1 \simeq 0.026$. This value and also the relaxation rate τ_1^{-1} are compatible with the corresponding values derived from ultrasonic experiments, which are $g \approx 0.03$ (Ref. 4) and $\langle \tau^{-1} \rangle_{av} \approx 2 \times 10^{11}$ sec^{-1} at $T \simeq 130$ K (Ref. 23), respectively.

D. Structural defects

In the following, we would like to discuss our data in view of the model of AHV.[5,6] This model can also provide physical pictures for the relaxation processes discussed above very generally. AHV assume that atoms or groups of atoms can have two equilibrium positions in a more or less asymmetric double-well potential (see Fig. 6). For defects where the asymmetry is quite large and the central barrier quite high, transitions between the upper and lower level can occur mainly through thermally activated jumping across the top of the barrier; at low temperatures, these defects are expected to be frozen. For defects where the asymmetry is small, transitions between the upper and lower level occur through phonon-assisted tunneling at low temperatures, and these two level states are believed to be responsible for the excess

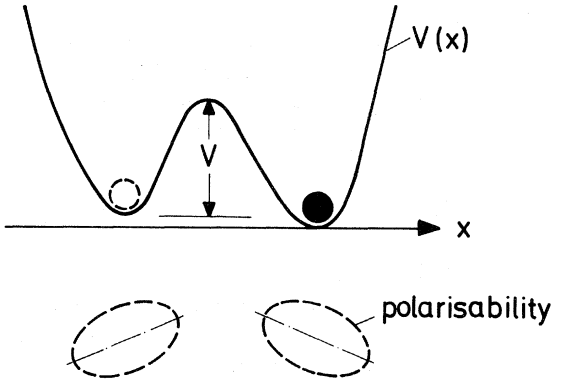

FIG. 6. Sketch of the double-well potential characterizing a structural defect; x is a generalized coordinate; when the atom undergoes a transition from one minimum to the other, the polarizability tensor may change its spatial orientation.

specific heat.[5,6] The first case has already been considered by Anderson and Bömmel[24] as a structural relaxation, in order to explain the ultrasonic absorption at temperatures $T > 30$ K; the second case has been considered by Jäckle[7,29] to account for the ultrasonic attenuation at temperatures $T < 20$ K. These relaxation processes can be seen in light scattering via their mechanical coupling to sound waves; however, there can also be a direct coupling of the structural defects to the light if the polarizability of a defect is anisotropic and does change its orientation or magnitude during a transition between the two levels.

Anderson and Bömmel[24] have suggested that the structural defects may involve the motion of oxygen atoms. It is known that the polarizability of oxygen in a compound is larger the larger the available volume for the oxygen.[31] Therefore, it seems to be possible that the polarizability of the oxygen in a double-well potential may be quite anisotropic; furthermore, the spatial orientation of the polarizability ellipsoid may depend on the location in the double well, as is sketched in Fig. 6.

The picture we try to develop here is similar to the situation found in liquids. If the polarizability of a molecule is isotropic, then we only see the polarized scattering from the density fluctuations, i.e., a Brillouin doublet and a central line; if, however, the polarizability is anisotropic, there is in the spectrum an additional contribution which is depolarized and whose spectral width may be much larger than the Brillouin frequency. This contribution is called the reorientational scattering or Rayleigh wing[20] and allows, if the molecules reorient independently from each other, the motion of an individual molecule to be seen. It corresponds to the incoherent neutron scattering, which also allows the study of the motion of an individual atom.

In order to see whether the defects can directly couple to the light with sufficient strength, we consider a very simple model. We approximate the structural defects by a gas of anisotropic molecules having rotational symmetry and being characterized by a certain anisotropy $\Delta\alpha$ of their polarizability. The integrated intensity of their reorientational scattering has been calculated in Appendix B and depends on $\Delta\alpha$ and on the number density of defects N_D. From the experimental data at 295 K, we have determined the ratio of the integrated "excess" scattering to the (polarized) Brillouin scattering to be 8.7×10^{-3}. Using $N_D = 10^{19}$ cm^{-3}, which should be an order-of-magnitude approximation for the number of thermally excited defects[2,5] at $T \approx 100$ K, we compute the anisotropic part of the polarizability to be $\Delta\alpha \simeq 10^{-24}$ cm^3. This number has to be compared with the polarizabilities of a SiO_2 unit and an O^{--} in SiO_2, which are 3×10^{-24} cm^3 or 1.7×10^{-24} cm^3, respectively.[31] Thus, it seems possible that the defects could directly couple to the light through an anisotropy of the polarizability; however, it appears less probable that a single oxygen can produce an anisotropy of the required magnitude; of course, this consideration is only qualitative, due to the uncertainty of N_D.

In principle, it appears possible that the light can directly induce transitions between the upper and lower level of a defect state. The frequency shift of the scattered light would correspond, in this case, to the energy difference ΔE of the two levels. Assuming a certain probability for such a transition, the scattering rates for energy loss and gain depend on the thermal population of the two levels. Considering levels with $\Delta E < 14$ cm^{-1}, i.e., $\Delta E < 20$ K, the scattering rates would hardly vary with temperature for $T > 2\Delta E$, i.e., $T > 40$ K. Our Raman spectra (see Fig. 4) however, do not indicate any contribution remaining fairly constant with temperature.

E. Conclusion

We have discussed the excess scattering in view of the structural defects being present in the glass. We have seen that the coupling of the defects to the light can occur in two ways: firstly, indirectly via the mechanical coupling of the defects to the sound waves, and secondly, via a direct coupling. The indirect coupling is already implied in the model used by Fulde and Wagner[4] for the discussion of the thermal anomalies; the direct coupling can arise through a mechanism suggested in this paper on the basis of the models of Anderson, Halperin, and Varmá[5] and of Anderson and Bömmel.[24] At present, it cannot be decided what type of coupling gives the dominant contribution to the scattering. Further experiments, extending to still lower tem-

peratures and including the Brillouin frequency region, should help to clarify this point; in particular, they could provide more precise information on the magnitude of the relaxation rates.

Stolen has already pointed out that the far infrared absorption α of fused quartz appears to arise from the same normal vibrations as the low-frequency Raman scattering[12,13] and that α/ω^2 has a similar spectral shape as the Raman scattering for $\omega < 120$ cm^{-1}. The absorption was found to be independent of temperatures[12,13,32] for $\omega > 20$ cm^{-1}, which is consistent with modes behaving like harmonic oscillators. However, the absorption was measured to decrease with decreasing temperature[12,32] for frequencies $\omega < 20$ cm^{-1}, just where, in our experiment, the excess Raman scattering is observed and also found to decrease with temperature. These facts suggest that the absorption for $\omega < 20$ cm^{-1} involves the same physical mechanisms responsible for the excess Raman scattering as discussed in this paper.

ACKNOWLEDGMENTS

The author gratefully acknowledges stimulating discussions with Professor M. Cardona, Professor K. Dransfeld, Professor P. Fulde, Professor L. Genzel, Professor J. Jäckle, Dr. A. Martin, Dr. T. P. Martin, and Dr. R. Zeyher. He has further benefitted from cooperation with Dr. I. Gregora during some of the low-temperature runs.

APPENDIX A

In this section, we would like to derive from the theory of Ref. 16 a value for the depolarization ratio of the amorphous Raman background. Using the notation of Ref. 16 and setting the terms with $D^i_{\beta\alpha\gamma\delta} = 0$, we obtain from Eq. (24) of Ref. 16 the depolarization ratio

$$\frac{I_{yzzy}}{I_{yyyy}} \simeq \frac{E_{yzzy}(l) + (v_l/v_t)^5 E_{yzzy}(t)}{E_{yyyy}(l) + (v_l/v_t)^5 E_{yyyy}(t)} , \tag{A1}$$

with

$$E_{yzzy}(l) \simeq \frac{C_t^2}{15}\left(\frac{\delta C_t^2}{C_t^2}\right) ,$$

$$E_{yzzy}(t) \simeq \frac{C_t^2}{10}\left(\frac{\delta C_t^2}{C_t^2}\right) ,$$

$$E_{yyyy}(l) \simeq C_l^2\left(\frac{\delta C_l^2}{C_l^2} + \lambda\right) + \frac{4C_t^2}{45}\left(\frac{\delta C_t^2}{C_t^2} + \lambda\right) ,$$

$$E_{yyyy}(t) \simeq \tfrac{2}{15} C_t^2\left(\frac{\delta C_t^2}{C_t^2} + \lambda\right) .$$

Here (l) and (t) refer to the scattering contributions of longitudinal and transverse sound waves, respectively. $(\delta C/C)^2$ and λ are a measure of the relative mean-square (spatial) fluctuation of the photoelastic constants and the elastic constants, respectively.

The ratio of the longitudinal to the transverse sound velocity v_l/v_t in fused quartz is given by $v_l/v_t = 1.57$, and the ratio C_l/C_t is related to the photoelastic (Pockels) constants p_{ij} (Ref. 33) of fused quartz by

$$\left|\frac{C_l}{C_t}\right| = \frac{p_{11}+2p_{12}}{3(p_{12}-p_{11})} = \frac{p_{12}-2/3(p_{44})}{2p_{44}} = 1.5 .$$

From Eq. (A1) and the above numbers, it can be seen that the depolarized scattering I_{yzzy} is dominated by the contribution of the transverse sound waves, which is stronger than the contribution of the longitudinal waves by a factor of $(v_l/v_t)^5 \tfrac{3}{2} = 15.64$. In the polarized scattering I_{yyyy}, the contributions of longitudinal and transverse sound waves are of the same order of magnitude when we assume, according to Ref. 16,

$$\delta C_l^2/C_l^2 \simeq \delta C_t^2/C_t^2 . \tag{A2}$$

Combining the above assumption with Eq. (A1), we obtain for the depolarization ratio in the long-wavelength limit, i.e., v/ω much greater than the correlation length ξ

$$\frac{I_{yzzy}}{I_{yyyy}} \simeq \frac{1}{10}\left(\frac{C_t}{C_l}\right)^2\left(\frac{v_l}{v_t}\right)^5 \times\left[\frac{1+\frac{2}{3}(v_t/v_l)^5}{1+[\frac{4}{45}+\frac{2}{15}(v_l/v_t)^5](C_t/C_l)^2}\right] . \tag{A3}$$

Inserting the numerical values for fused quartz, we obtain $I_{yzzy}/I_{yyyy} \simeq 0.28$. Note that this value is considerably larger than the depolarization ratio of the Brillouin scattering from transverse and longitudinal sound waves, which is given[20] by

$$I_t/I_l = \tfrac{1}{2}(p_{44}/p_{12})^2(v_l/v_t)^2 = 0.094 .$$

APPENDIX B

In the following, we shall consider the reorientational scattering from a gas composed of molecules being characterized by the following tensor polarizability:

$$\alpha_{ij} = \begin{pmatrix} \alpha_0 & 0 & 0 \\ 0 & \alpha_0 & 0 \\ 0 & 0 & \alpha_0+\Delta\alpha \end{pmatrix} = \alpha_0\delta_{ij} + \Delta\alpha \begin{pmatrix} 0 & 0 & 0 \\ 0 & 0 & 0 \\ 0 & 0 & 1 \end{pmatrix} .$$

The scalar part of α_{ij} is responsible for the scattering from the density fluctuations, whereas the tensor part $\Delta\alpha$ gives rise to the reorientational scattering. Assuming uncorrelated reorientation, the scattering contributions due to $\Delta\alpha$ add up incoherently and have a depolarization ratio[20] of $\frac{1}{3}$.

The average power radiated within the solid angle $d\Omega$ by one dipole $\vec{p}$ is given by

$$dP_{\text{scatt}}(t) = (1/4\pi c^2)\,|\ddot{\vec{p}}|^2 \sin^2\phi\, d\Omega , \tag{A4}$$

where c is the velocity of light, and ϕ is the angle between $\vec{p}$ and the propagation direction of the radiated light. The average mean-square dipole moment p_z, induced by an oscillating local field $E_{0z\,\mathrm{eff}}$ and due to $\Delta\alpha$, is given by[20]

$$\langle P_z^2(t)\rangle = \tfrac{3}{15}\Delta\alpha^2 E_{oz\ \mathrm{eff}}^2(t) \qquad \text{(A5)}$$

Inserting the above relation into Eq. (A4) and using $E_{oz\ \mathrm{eff}} = \frac{1}{3}E_0(\epsilon+2)$, we obtain for the power of the polarized reorientational scattering integrated over all frequency shifts

$$dP_{\mathrm{scatt}} = P_0\left(\frac{\omega_0}{C}\right)^4 \frac{3}{15}(\Delta\alpha)^2\left(\frac{\epsilon+2}{3}\right)^2 \sin^2\phi N_D\, L d\Omega\,, \qquad \text{(A6)}$$

where P_0 is the incident power, $\omega_0/2\pi$ is the frequency of the incident light, ϵ is the dielectric constant at ω_0, N_D is the number density of molecules, and L is the scattering length.

The spectral width of the reorientational scattering is determined by the average reorientation rate and may be quite large in comparison to the characteristic Brillouin frequency. The ratio of this scattered power relative to the light power dP_{Brill} (Ref. 34) scattered by longitudinal sound waves within the same solid angle $d\Omega$ is

$$\frac{dP_{\mathrm{scatt}}}{dP_{\mathrm{Brill}}} = \frac{3}{15}(\Delta\alpha)^2\left(\frac{\epsilon+2}{3}\right)^2 \frac{(4\pi)^2\rho_0 v_l^2}{n^8 p_{12}^2 kT} N_D\,. \qquad \text{(A7)}$$

*An account of this work was reported at the Second Conference, Cond. Matt. Div. of the European Physical Society, Budapest, 1974.

[1]R. C. Zeller and R. O. Pohl, Phys. Rev. B 4, 2029 (1971).

[2]R. B. Stephens, Phys. Rev. B 8, 2896 (1973).

[3]J. C. Lasjaunias, R. Maynard, and D. Thoulouze, Solid State Commun. 10. 215 (1972).

[4]P. Fulde and H. Wagner, Phys. Rev. Lett. 27, 1280 (1971).

[5]P. W. Anderson, B. I. Halperin, and C. M. Varma, Philos. Mag. 25, 1 (1972).

[6]W. A. Phillips, J. Low Temp. Phys. 7, 351 (1972).

[7]J. Jäckle, Z. Phys. 257, 212 (1972).

[8]W. Heinicke, G. Winterling, and K. Dransfeld, in *Proceedings of the Second International Conference on Light Scatterings in Solids*, edited by M. Balkanski (Flammarion, Paris, 1971).

[9]S. Hunklinger, W. Arnold, S. Stein, R. Nava, and K. Dransfeld, Phys. Lett. A 42, 253 (1972); B. Golding, J. E. Graebner, B. I. Halperin, and R. J. Schutz, Phys. Rev. Lett. 30, 223 (1973).

[10]W. F. Love, Phys. Rev. Lett. 31, 822 (1973).

[11]P. Flubacher, A. J. Leadbetter, J. A. Morrison, and B. P. Stoicheff, J. Phys. Chem. Solids 12, 53 (1959); M. Tobin and T. Baak, J. Opt. Soc. Am. 58, 1459 (1968).

[12]R. H. Stolen, Phys. Chem. Glasses 11, 83 (1970).

[13]M. Hass, J. Phys. Chem. Solids 31, 415 (1970); Solid State Commun. 7, 1069 (1969).

[14]E. Whalley and J. E. Bertie, J. Chem. Phys. 46, 1264 (1967).

[15]R. Shuker and R. W. Gammon, Phys. Rev. Lett. 25, 222 (1970).

[16]A. Martin and W. Brenig, Phys. Status Solidi B 64, 163 (1974).

[17]Manufacturer: Hereaus-Schott Quarzschmelze, 645 Hanau, West Germany.

[18]The low-frequency Raman scattering from amorphous silicon has only been measured for frequency shifts $\omega > 20$ cm^{-1}, see J. S. Lannin, Solid State Commun. 12, 947 (1973).

[19]T. C. Rich and D. A. Pinnow, Appl. Phys. Lett. 20, 264 (1972).

[20]I. L. Fabelinskii, *Molecular Scattering of Light* (Plenum, New York, 1968).

[21]The lowest Raman line in crystalline quartz ($q \approx 0$) is found at 128 cm^{-1}.

[22]$\xi = 6.4$ Å corresponds to the r value at which the last peak was observed in the measured pair function distribution curve of vitreous silica; see, R. L. Mozzi and B. E. Warren, J. Appl. Crystallogr. 2, 164 (1969). The transverse sound velocity v_t was taken to be 3.7×10^5 cm/sec to obtain a numerical estimate for the upper frequency limit of the continuum approximation.

[23]A. S. Pine, Phys. Rev. 185, 1187 (1969). The linewidth data of Pine obtained at a frequency shift $\omega/2\pi \approx 26.8$ GHz show a pronounced maximum at $T \approx 130$ K. According to relaxation theory, the relaxation rate $\tau^{-1} = \omega$ at this temperature.

[24]O. L. Anderson and H. E. Bömmel, J. Am. Ceram. Soc. 38, 125 (1955).

[25]P. C. Martin, in *Many Body Physics*, edited by C. de Witte and R. Balian (Gordon and Breach, New York, 1968).

[26]J. Sandercock (private communication).

[27]For $\omega > 20$ cm^{-1}, the temperature dependence of the scattering is found to be consistent with one-phonon processes.

[28]S. Hunklinger, W. Arnold, and S. Stein, Phys. Lett. A 45, 311 (1973).

[29]J. Jäckle, report (unpublished).

[30]For this estimate, the high-frequency cutoff was chosen to be $\omega_0 = 120$ cm^{-1}, which is just below the lowest optical phonon of crystalline quartz.

[31]J. R. Tessman, A. H. Kahn, and W. Shockley, Phys. Rev. 92, 890 (1953).

[32]P. T. T. Wong and E. Whalley, Discuss. Faraday Soc. 50, 94 (1970).

[33]W. Primak and D. Post., J. Appl. Phys. 30, 779 (1959); J. Schroeder *et al.*, J. Am. Ceram. Soc. 56, 510 (1973).

[34]G. B. Benedek and K. Fritsch, Phys. Rev. 149, 647 (1966).